

Efficiency of a new steel hysteretic device for an intermediate seismic isolation system applied to reticular domes

Shiro KATO^{*}, Takanori OYA^a, Shoji NAKAZAWA^b, and Yun-Beom KIM^a

^{*} Prof. Department of Architectural and Civil Engineering, Toyohashi University of Technology, Tempaku, Toyohashi 441-8580. Japan
E-mail kato@tutrp.tut.ac.jp

^a Senior Engineer, Tomoe Corporation,

^b Professor, Toyohashi University of Technology

Abstract

The present paper discusses the efficiency of a new steel hysteretic device, abbreviated as “J-damper”, proposed for an intermediate seismic isolation system of spatial structures. In order to show the effectiveness, a series of dynamic response analyses of single layer reticular domes are performed considering wave passage effects. From the energy consumption concept, it is shown that the intermediate seismic isolation system much suppresses the seismic responses of the dome and the new device can exert their excellent performance irrespective of a spatial variation of earthquake input motions.

Keywords: J-damper, steel hysteretic device, earthquake response, wave passage effects, energy consumption, efficiency

1. Introduction

Recently, a considerable progress has been made in the studies on the application of intermediate seismic isolation system to spatial structures, since it is regarded as one of the most effective systems, and this kind of concepts was explained by several researches[1-3] also in the previous paper by authors[2,3]. The present paper discusses the efficiency of a new steel hysteretic device, called here as J-dampers, for the intermediate seismic isolation system [ISIS for abbreviation]. In this paper the former preliminary work [3-5] is extended with a more elaborate study of absorbed energy in the devices considering wave passage effects of earthquake motions. In order to show its effectiveness even at a site with wave passage effects or irregular soil conditions[6,7], a series of dynamic response analyses of a reticular dome with and without new hysteretic devices are performed. And it is revealed that the new devices can exert their excellent performance under severe soil and seismic conditions.

2. Analytical model, overall geometry and member properties

The global geometry is shown in Fig.1. The structure is composed of four parts: a single layer reticular steel dome, an intermediate seismic isolation system (here abbreviated to ISIS), a reinforced concrete (RC) substructure and a foundation system. The dome has a medium size with 100m as a diameter of plan, 40 degrees as a half open angle of ϕ_d , and 2.0 degrees as a half-subtended angle θ for members. Along the ridge line AOA', there are twenty beam-column members with a constant length $l_0 = 5.43\text{m}$ and the members with 40 as member slenderness ratio λ_0 are rigidly connected at nodes. The ISIS with 1.0m in height has J-dampers together with friction dampers, whose characteristics are mentioned later. The substructure with 5.0 m as height it is made of reinforced concrete. It has totally 60 RC columns with a solid circular section, and a ring girder connecting them at top level with a solid rectangular section. The foundation system has pre-cast (PC) piles with 45cm in diameter and a rectangular foundation beam with the sectional size of 250.0cm \times 100.0cm. Two PC piles support each footing of the column with the foundation

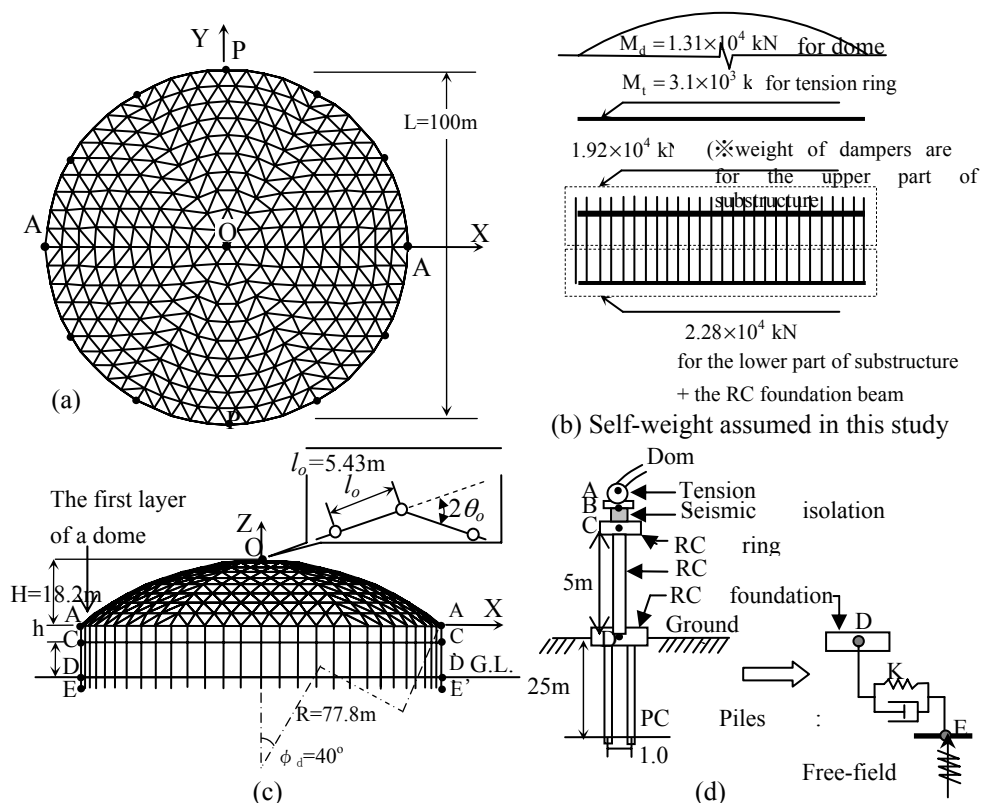


Figure. 1 Analytical model of a spatial structure

beam, which connects all pile heads circumferentially, as shown in Fig.1(d). Table.1 lists the properties of all structural members. The Young's and shear moduli are assumed to be 20580.0 and 7938.0kN/cm² for steel and 2058.0 and 882.0kN/cm² for reinforced concrete, respectively. The yield stress of steel is 23.5 kN/cm². The dome is made up of steel pipes with a hollow circular section.

Table.1 Properties of structural members

member	size	A (cm ²)	I _y (cm ⁴)	I _z (cm ⁴)
Hoop	φ 355.6×8 mm (steel pipe)	87.4	1.32×10 ⁴	1.32×10 ⁴
diagonal and ridge	φ 355.6×6.3 mm (steel pipe)	69.1	1.05×10 ⁴	1.05×10 ⁴
Tension ring	φ 700.0×14.0 mm (steel pipe)	301.7	1.78×10 ⁵	1.78×10 ⁵
Ring girder	250 cm×60 cm (RC)	15000.0	4.50×10 ⁶	7.81×10 ⁷
Column	φ 100 cm (RC)	7854.0	4.91×10 ⁶	4.91×10 ⁶
Foundation beam	250 cm×100 cm (RC)	25000.0	2.08×10 ⁷	1.30×10 ⁸

In order to obtain the numerical results reflecting the wave passage effects due to the spatial variation of the surface earthquake motion, the piles connected with the foundation beam are modeled with the equivalent elastic shear spring elements reflecting the soil-pile interaction as shown in Fig.1(d).

The self-weight distribution of a spatial structure is given in Fig.1(b). The weight per unit surface area of the dome except for the tension ring is assumed to be 1.77 kN/m² and the weight per unit volume of reinforced concrete elements is assumed to be 24.0kN/m³.

In order to confirm the efficiency of J-dampers, two models with and without the ISIS are adopted in this research. These two models are called “a conventional model” and “a seismic isolation model”, respectively. As the boundary condition for the seismic isolation model, it is assumed that the translational degrees of freedom in the Z direction are restrained at the both levels of tension ring and ring girder. The rotational degrees of freedom in the X and Y direction are also restrained at the nodes on the ring girder to avoid its out-of-plane bending deformation.

3. Intermediate seismic isolation system using J-dampers

The configuration of a set of the J-damper is illustrated in Figs.2 and 3. One J-damper is composed of four J-plates together with some necessary components. Plastic deformation of J-plates is exerted through their stable rolling-bending motions under the restraint by slide plates and guide frame, and this behavior makes it possible for them to effectively dissipate seismic energy and to form stable hysteretic loops with large displacement amplitudes.

As illustrated in Figs.1 and 2, 60 sets of J-dampers are interposed between the dome and the substructure (ring girders) together with friction dampers, each corresponding to each column. They work only against horizontal displacements in the circumferential direction

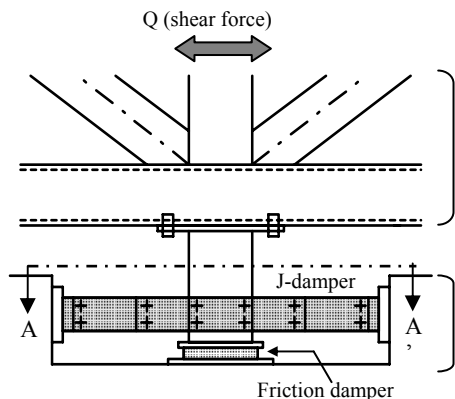


Figure. 2 Installation configurations of J-dampers and friction dampers

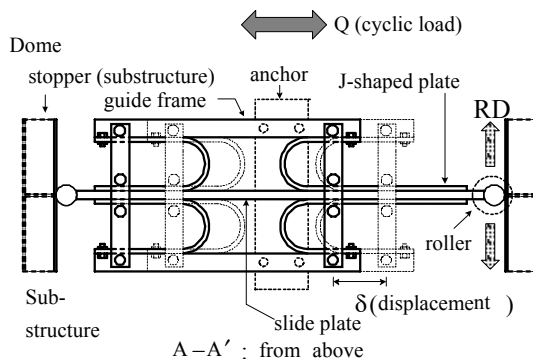


Figure. 3 Configuration of a set of J-damper

along the ring girder, while they move freely on their rollers in the direction perpendicular to the ring girder, and the thermal stresses due to expansion of the steel dome are released under temperature changes.

Prediction of the elastic stiffness, yield strength and strain-hardening slope of one J-plate was suggested in Ref. [3,4] and the details are abbreviated here. The characteristics of friction dampers are assumed as MSS model (a multiple shear spring model), and the total friction forces Q_Y^f are proportional, as expressed as $Q_Y^f = \mu^f \times N^f$, to the total normal forces N^f acting on the interface, where μ^f and N^f represent the friction coefficient and the normal forces, respectively. The normal force N^f is assumed as 269.2 kN. The effects of variation of the friction coefficient on the seismic responses of the structure and the J-dampers need to be investigated, but the friction coefficient is assumed to be constant, $\mu^f = 0.1$, in this study. Therefore, the friction tangential forces Q_Y^f is taken as 26.9 kN for response analysis in the present study.

4. Input earthquake motion

Fig.4 shows the analytical model for wave passage effects [6,7] to consider the spatial variation of earthquake motions at the ground surface. In this study, the model is subjected to a SH-wave motions propagating in Y-direction inputted in engineering bed rock with an wave incident angle, ϕ . Local irregularity of soil layers at site is neglected. The time delay ΔT occurs between two points A1 and A2, due to the wave passage effect, and is represented by the shear wave velocity of engineering bed rock V_s and the incident angle ϕ as follows.

$$\Delta T = \frac{L \sin \phi}{V_s} = \frac{L}{V_c} \quad , \quad V_c = \frac{V_s}{\sin \phi} \quad (1)$$

where V_C is the apparent shear wave velocity and V_S is assumed to be 400 m/sec. Values of 0, 15, 30 and 45degrees are assigned for ϕ in order to grasp the effect of ϕ on the seismic responses. Considering this condition, as an input earthquake motion on the ground surface in X-direction, the scaled El-Centro (1940) NS earthquake signal normalized for peak ground acceleration A_{max} of 500cm/sec² is adopted

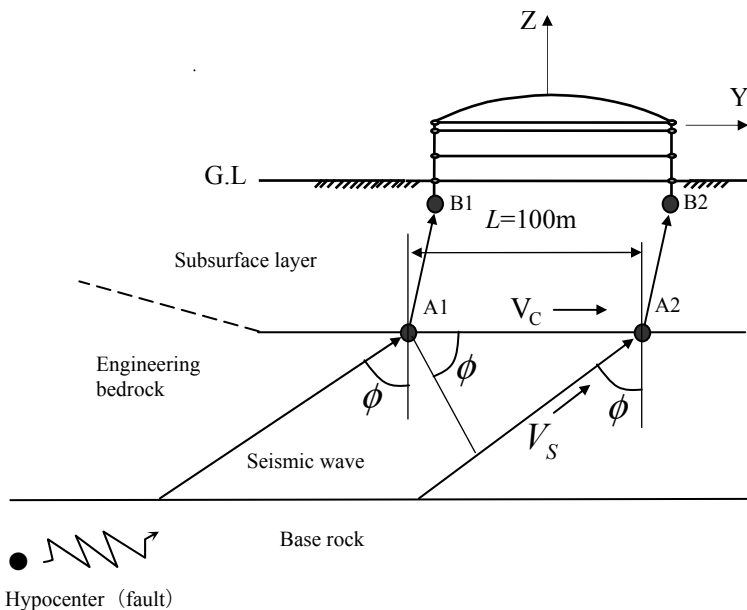


Figure.4 Model of the dome subjected to a traveling wave in the Y direction

5. Effectiveness of J-damper in case of no consideration of wave passage effects

5.1 Acceleration responses of spatial structure

Fig.5 demonstrates the distribution of maximum horizontal and vertical acceleration responses of nodes located along the central ridge line including the substructure (E-A-O-A'-E' line given in Fig.1). The variable, α_Y^d , denotes the base shear coefficient of the total J dampers installed at the top of substructure, accordingly leading a condition that the total resisting shear coefficient for the total shear force at the top of the substructure is 0.2 due to adding the contribution of friction dampers.

The maximum horizontal and vertical acceleration responses of nodes located along the central ridge line (A-O-A') are around 1300.0 cm/sec² and 500.0~900.0 cm/sec² for conventional model, and responses of the dome for seismic isolation model with $\alpha_Y^d = 0.1$ are reduced to about 1/3 of those of the conventional model. Reduction rates become more prominent when α_Y^d becomes lower. But, maximum horizontal acceleration responses of

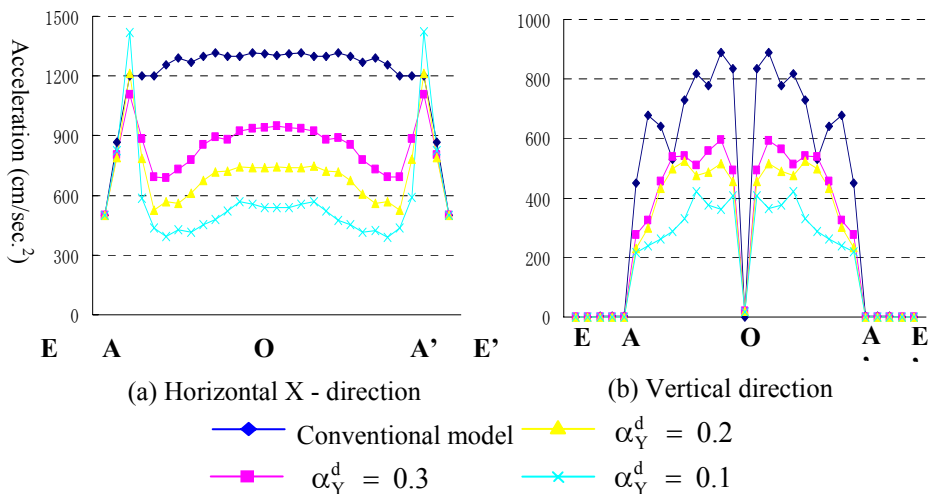


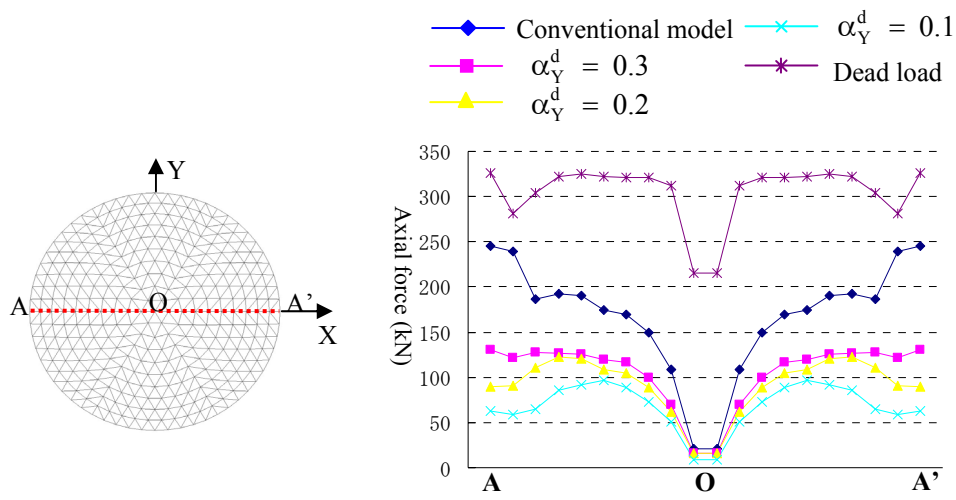
Figure.5 Distributions of maximum acceleration responses (ABS)
 (※ ABS is an abbreviation for absolute value)

the substructure remain almost the same for both models.

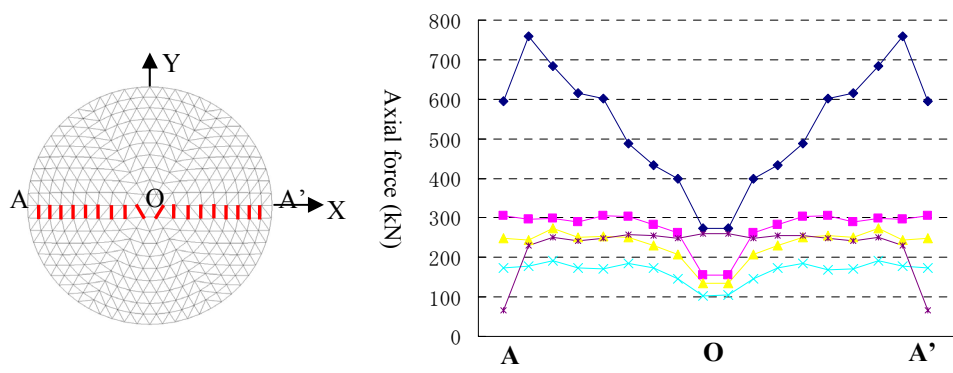
Therefore, introduction of the ISIS with J-dampers and friction dampers enables the dome structure to reduce horizontal and vertical acceleration responses effectively, when subjected to strong horizontal earthquake. This characteristics may lead to the safety of the structure itself. Further, it would minimize the damages to nonstructural components such as suspended ceilings, lights and acoustic facilities, because fall-down of such items spoils the safety of its interior space. However, reduction of acceleration responses for the substructure is not expected.

5.2 Axial forces in dome members

Fig. 6 demonstrates the distribution of maximum axial forces in dome members, which exclude the axial forces due to dead load. It can be seen that the ISIS with a lower value of α_Y^d exerts a great reduction in their axial forces. The dome member forces of the conventional model are largely amplified due to severe earthquake motions, and members will be plasticized or buckled if no measures are taken to increase the sectional areas. This amplification of the forces will make construction cost high in order to satisfy the present design policy as it specifies that any members in reticular domes shall remain in elastic range. The results of seismic isolation model show clearly that ISIS makes it possible for members to remain in elastic range under a severe earthquake and their sectional sizes could be reduced, leading to the realization of a light-weight dome and curtailment of its construction cost.



(a) Ridge members ($N_Y = 1624.6\text{kN}$)



(b) Hoop members ($N_Y = 2053.0\text{kN}$; not including tension ring members)

Figure.6 Distributions of maximum axial forces for dome members (ABS)
 (※ N_Y denotes a yield axial force)

5.3 Evaluation of behavior of ISIS and hysteretic dampers based on energy concept

In this section, seismic responses of ISIS and hysteretic dampers are investigated from the perspective of energy concept on the premise that the wave passage effect is neglected.

When a structure is subjected to an earthquake motion, some portion of the input energy E , imposed on a structure by the seismic event is stored temporarily in the structure as kinetic energy W_K and fully recoverable elastic strain energy W_S , while the rest must balance the dissipative energy caused by inherent damping within the structure W_h and its dissipative plastic strain energy W_p . Replacing the sum of W_K and W_S by the elastic vibration energy W_E , the energy balance equation can be expressed by

$$W_E + W_h + W_p = E \quad (2)$$

in which W_p is assumed separable into additive contributions W_p^d and W_p^f , representing the energy dissipated by the J-dampers and the friction dampers, respectively.

Fig.7 shows the occupation ratio of the individual energy components balancing total input energy imparted to a spatial structure through the duration of a seismic disturbance with respect to α_Y^d . A significant portion of the input energy is consumed by inelastic hysteretic mechanism of J-dampers and friction dampers. The total energy dissipated by J-dampers and friction dampers, $W_p^d + W_p^f$, has the constant value of around 70% of the total input energy, irrespective of α_Y^d . With the increase in α_Y^d , even an greater share of the energy tends to be dissipated via inelastic deformation of the J-dampers rather than the friction dampers. Therefore, it can be noticed that the energy input into the dome from the seismic disturbance is much reduced with the addition of the ISIS, leading to the reduction of the seismic responses of the dome identified in the prior sections.

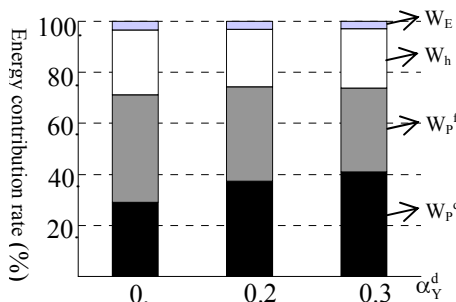


Figure.7 Energy contribution rate of each part of the structure

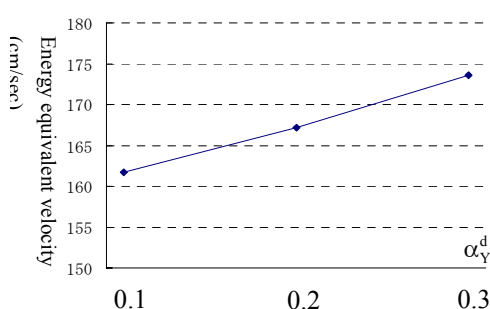


Figure.8 Energy equivalent velocity V_E

Fig.8 shows relation between α_Y^d and energy equivalent velocities V_E defined by the following equation

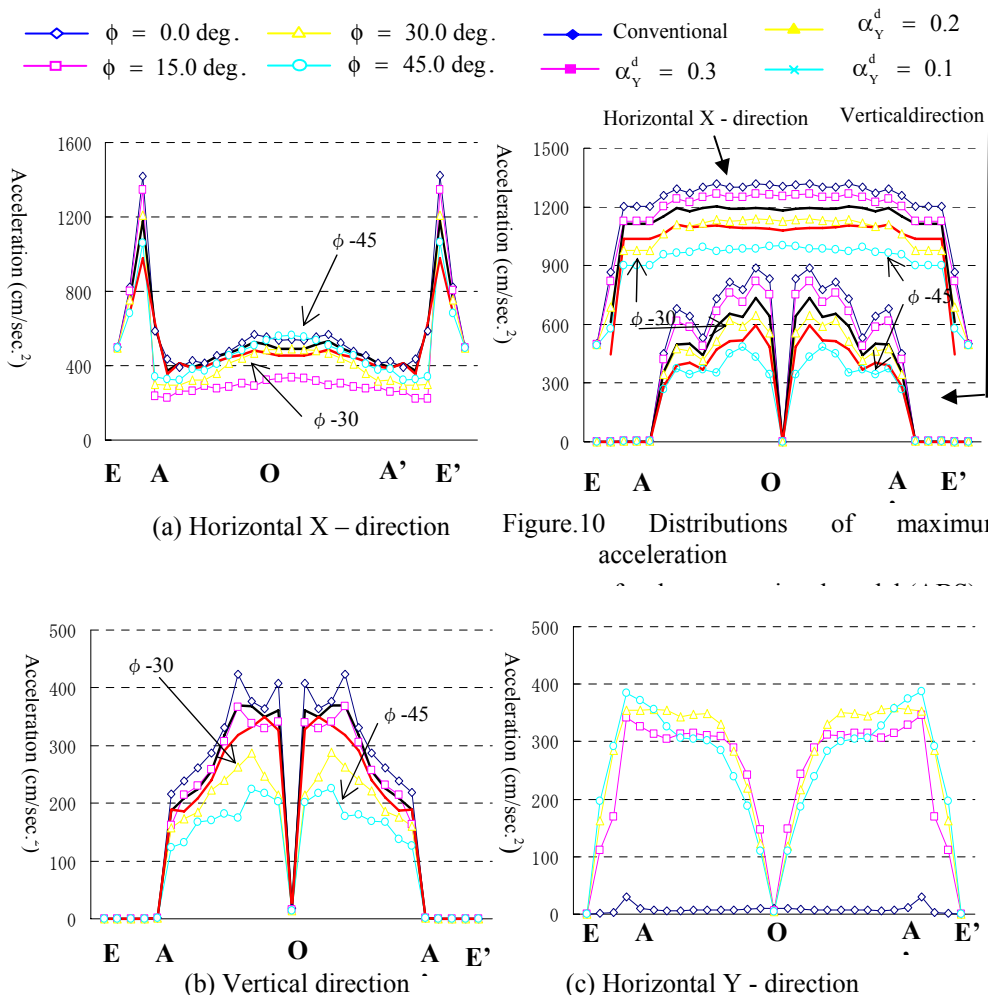
$$V_E = \sqrt{2E / M_{total}} \quad (13)$$

where M_{total} denotes the total mass of the structure. V_E increases slightly with raising α_Y^d and ranges from 160.0 to 170.0 cm/sec. From Figs. 7 and 8, it can be seen that, although the input energy has increased slightly, the dampers consume a significant portion of the total energy, thus protecting the primary structure.

6. Effectiveness of J-dampers in case of considering wave passage effects

6.1 Acceleration responses of spatial structure

Fig. 9 shows the distributions of absolute maximum horizontal and vertical acceleration responses for nodes on the central line (E-A-O-A'-E') of the dome and substructure for different ϕ when $\alpha_Y^d = 0.1$. Fig. 10 shows the results for the conventional model. From



(a) Horizontal X – direction

Figure.10 Distributions of maximum acceleration

(b) Vertical direction

(c) Horizontal Y - direction

Figure.9 Distributions of maximum acceleration

responses for the seismic isolation model ($\alpha_Y^d = 0.1$; ABS)

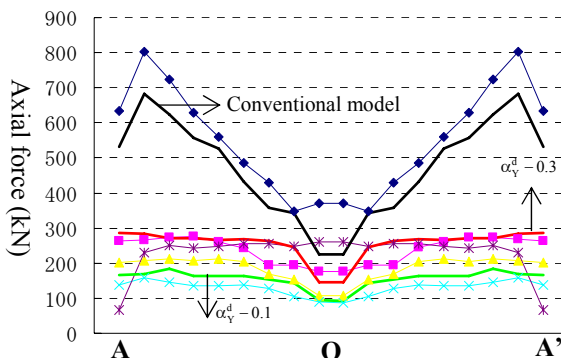


Figure.11 Distributions of maximum axial forces for hoop members (ABS) (not including tension ring members) $\phi = 30.0$ deg.

Figs.9 and 10, it can be found that maximum horizontal and vertical acceleration responses of the dome for the seismic isolation model decrease appreciably in comparison with the conventional model. The results indicate that the ISIS with J-dampers is very effective in reducing the acceleration responses of the dome even when wave passage effects are considered. However, reduction of acceleration responses for the substructure was not found, although the data are not shown in this study.

The results also show clearly that maximum acceleration responses for these two models are much dependent on the wave incident angle ϕ . Fig. 10 explains maximum horizontal and vertical acceleration responses for the conventional model reduce as the angle increases. As we can see from Fig. 9, both the vertical accelerations of the dome and the horizontal accelerations of the substructure drop with the increase in ϕ for the seismic isolation model.

6.2 Axial forces in dome members

Fig.11 demonstrates an example that maximum axial forces in dome members of the seismic isolation model reduce greatly with the drop of α_Y^d in comparison with the conventional model in the case of $\alpha_Y^d = 0.1$ and an incident angle of $\phi = 30.0^\circ$, while other cases are abbreviated. The values of the distribution exclude the axial forces due to dead load.

Although other data are abbreviated, the results reveal that the ISIS with J-dampers can greatly reduces stress responses and acceleration responses irrespective of wave passage effects.

7. Conclusion

The present paper discussed the efficiency of a new steel hysteretic device for an intermediate seismic isolation system of a spatial structure. The system composed of the steel devices and friction dampers is interposed between a dome and a substructure. Through a series of dynamic response analyses of conventional and seismic isolation models, it has been confirmed that irrespective of the wave passage effects caused by a spatial variation of input earthquake motions, the proposed dampers effectively suppress the responses of a spatial structure.

Acknowledgement

The present authors would like to express great thanks to Drs. T Okamoto, T Ueki, T Yamashita, and L Su for their encouragements to the present study, since the present research is an extension from the joint works [3-7] previously performed together with them.

References

- [1] Kumagai T., Takeuchi T., Ogawa T., Nakama A. and Sato E. "Seismic response evaluation of latticed domes with elasto-plastic substructures using amplification factors", IASS symposium, 2005, Bucharest in Rumania, 383-390.
- [2] Kato S., Nakazawa S., Minegishi T. and Uchikoshi M. "On how the assumption of damping matrix effects on the earthquake responses of large reticulated domes – comparison between Rayleigh damping and stiffness-proportional damping", Journal of Structural Engineering, AIJ, 1999, Vol. 4bB, 159-171 [in Japanese].
- [3] Kato S., Nakazawa S., Matsushita F., Ohya T. and Okamoto T. "A new system of intermediate isolation for space structures against earthquakes", Fifth International Conference on Space Structures, 2002, London in UK, 1053-1062.
- [4] Kato S., Kim Y.-B., Nakazawa S. and Ohya T. "Simulation of the cyclic behavior of J-shaped steel hysteresis devices and study on the efficiency for reducing earthquake responses of space structures", Journal of Constructional Steel Research, 2005, Vol.61, 1457-1473.
- [5] Kato S. and Kim Y.-B. "A finite element parametric study on the mechanical properties of J-shaped steel hysteresis devices", Journal of Constructional Steel Research, 2006, Vol.62, 802-811.
- [6] Kato S. and Su L. "Effects of surface motion difference at footings on the earthquake responses of large-span gable structures", Steel Construction Engineering, JSSC, 2002, Vol.9, 113-128.
- [7] Kato S., Nakazawa S. and Su L. "Effects of wave passage and local site on seismic responses of a single layered reticular dome structure", Steel Construction Engineering, JSSC, 2003, Vol.10, 91-106.